Received: 17 November 2021 | Revised: 29 May 2022 | Accepted: 10 June 2022

DOI: 10.1111/eff.12673

Ecology of FRESHWATER FISH WILEY

ORIGINAL ARTICLE

The incorporation of environmentally derived $^{87}Sr/^{86}Sr$ and Sr/Ca in early otolith formation of Chinook salmon

Paul Chittaro[1] | Jens Hegg[2] | Abby Fuhrman[1] | Devin Robichaux[3] | Rothboury Doung[4] | Brian Beckman[1] | Chris Fisher[5] | Jeff Vervoort[6] | Brian Kennedy[2]

[1]Environmental and Fisheries Sciences Division, Northwest Fisheries Science Center, National Oceanic and Atmospheric Administration, Seattle, Washington, USA

[2]Department of Fish and Wildlife Resources, University of Idaho, Moscow, Idaho, USA

[3]Civil & Environmental Engineering, University of Washington, Seattle, Washington, USA

[4]The Hans Rosling Center for Population Health, University of Washington, Seattle, Washington, USA

[5]School of Earth Sciences, The University of Western Australia, Crawley, Western Australia, Australia

[6]School of the Environment, Washington State University, Pullman, Washington, USA

Correspondence
Paul Chittaro, Environmental and Fisheries Sciences Division, Northwest Fisheries Science Center, National Oceanic and Atmospheric Administration, 2725 Montlake Blvd. E, Seattle, WA 98112, USA.
Email: paul.chittaro@noaa.gov

Funding information
Bonneville Power Administration

Abstract

Effective species management often requires understanding patterns of movement and habitat use. A common approach in identifying where individuals reside relies upon chemical tracers from the environment that are incorporated into an individual's tissues. For fish, isotopes in their otoliths, specifically the portion of their otolith formed during their larval stage, have been used to identify the natal origin. Complicating this work, however, is the fact that during this life stage, there is a shift in the source of isotopes deposited onto the growing otolith from maternally to environmentally derived. The objective of this study was to identify the portion of the otolith representing this transition to environmentally derived isotopes so as to accurately investigate questions of natal origin for a threatened population of fall Chinook salmon (*Oncorhynchus tshawytscha*). We exposed developing larvae to four treatments that differed in terms of their water strontium isotope ratio ($^{87}Sr/^{86}Sr$) and used change-point analysis of otolith $^{87}Sr/^{86}Sr$ and strontium to calcium ratio (Sr/Ca) to identify the otolith radius corresponding to the transition to environmentally derived isotopes. Our results indicated this transition occurred, on average, at 132 μm ($^{87}Sr/^{86}Sr$; ±50 μm standard deviation) and 127 μm (Sr/Ca; ±29 μm) from the otolith core, which corresponded to the developmental time between hatching and exogenous feeding. A substantial proportion of our otoliths (i.e., 61%) did not show convergence between otolith and water $^{87}Sr/^{86}Sr$ by the end of the 113-day experiment, which was likely due to the dietary contribution of marine-based feed. Therefore, we were unable to recommend an otolith radius to target for the purposes of reconstructing natal origin apart from being beyond approximately 130 μm.

KEYWORDS
change-point analysis, isotopes, natal location, otolith, trace element

1 | INTRODUCTION

Effective species management and conservation often require understanding patterns of movement and habitat use. A common approach used in identifying where individuals reside relies upon chemical tracers from the environment that are incorporated into an individual's tissues. These chemical tracers, such as stable isotopes and trace elements, are used as a location-specific marker and depending on the tissue being examined can represent a variety of temporal scales from days (blood, Kurle & Gudmundson, 2007) and

months (muscle, Elsdon et al., 2010), to years (baleen, Schell, 2000; vertebrae, Mohan et al., 2018; teeth, Hamilton & Evans, 2018).

For research on fish residence, otoliths (i.e., ear stones) are commonly used because of their unique chemical and physical properties. Specifically, otoliths are chemically inert and incorporate different elemental isotopes, many of which are environmentally derived (Walther & Thorrold, 2008), onto the growing surface of the otolith. Further, otoliths contain microstructural patterns of visible increments that are regularly added throughout the life of an individual (Stevenson & Campana, 1992). Together these chemical and microstructural properties of otoliths permit the retrospective reconstruction of where individuals resided and for how long (Brennan & Schindler, 2017; Johnson et al., 2012; Limburg et al., 2015; Walther, 2019).

Identifying the natal origin of fish has been a prominent research goal especially as the technologies and methods associated with measuring chemical tracers in otoliths have improved and become more accessible (Walther, 2019). Using the chemical properties of otoliths to reconstruct the natal origin, however, can be complicated because the isotopes incorporated into the core of the otolith, which represents otolith material formed prior to and at hatching, are not entirely derived from the environment. For example, several studies examining the otolith core have reported elevated concentrations of trace elements (Brophy et al., 2004; Chittaro et al., 2006; Michibata & Hori, 1979; Ruttenberg et al., 2005). The source of these elevated levels of elements has been suggested to be maternally derived and likely transferred to the developing embryo via its yolk sac (Kalish, 1990; Volk et al., 2000; Waite et al., 2008).

Studies interested in reconstructing natal origin, therefore, typically avoid the otolith core and instead target a portion of the larval otolith in which the isotopes of interest are assumed to be environmentally derived (Barnett-Johnson et al., 2008; Hegg, Kennedy, Chittaro, & Zabel, 2013). In particular, the developmental stages associated with hatching and first exogenous feeding, both of which are represented as visual marks on otoliths (Barnett-Johnson et al., 2007; Campana, 1992), are often used as landmarks on the otolith coinciding with the shift from maternally to environmentally derived isotopes (Barnett-Johnson et al., 2008). Recent work by Hegg et al. (2018) using trace element and stable isotope otolith analyses of juvenile Chinook salmon provided evidence supporting the shift to an environmentally derived source of isotopes occurring at the hatching and first exogenous feeding stages. Specifically, they observed a shift in strontium ($^{87}Sr/^{86}Sr$) and several elemental ratios (i.e., Mn/Ca and Ba/Ca) at a distance from the otolith core of 150 and 225 μm respectively.

The objective of this study was to identify, through an experimental approach, the portion of the otolith representing the transition to environmentally derived isotopes (e.g., strontium isotopes). Knowing where this transition occurs is important because studies increasingly rely upon detailed early life-history information. In this study, we conducted an exposure experiment in which developing hatchery fall Chinook salmon (*Oncorhynchus tshawytscha*) from the Snake River of Idaho (a tributary of the Columbia River in the U.S. Pacific Northwest) were placed in four treatments of water of known strontium isotope ratio ($^{87}Sr/^{86}Sr$) and raised for over three months from fertilised eggs to fry. Our experimental design permitted us the opportunity to investigate the assumption that a developing egg is a chemically closed system prior to yolk sac absorption and first feeding (Volk et al., 2000). If the egg is a closed system, then we expect stable isotope values to be constant in the portion of the otolith formed prior to yolk sac absorption and first feeding, and we would expect similarity in stable isotope values among treatments because the eggs used in our experiment were taken from females collected in the same river. We hypothesised that individual otolith transects would show $^{87}Sr/^{86}Sr$ values that shift towards the $^{87}Sr/^{86}Sr$ values of each water treatment at approximately 150 μm from the otolith core, and reach equilibrium after 250 μm (as was reported by Hegg et al., 2018). The overarching goal of this project was to increase our understanding of the accurate interpretation of otolith chemical records that are being increasingly employed for questions of fish natal origin and early life history. For species that are threatened or endangered under the Endangered Species Act (ESA), such as Snake River fall Chinook salmon, answers to these questions can inform both conservation actions and management decisions.

2 | METHODS

2.1 | Experimental setup

On November 20, 2017, we obtained milt and approximately 5000 unfertilized eggs of fall-run Snake River Chinook salmon from two sacrificed adult males and females, respectively, that were collected as part of spawning operations at Lyons Ferry Hatchery, Idaho (Oakerman et al., 2020). On the same day, we also collected approximately 130 L of water from each of three rivers known to differ in their water strontium isotope composition (Hegg, Kennedy, Chittaro, & Zabel, 2013): Tucannon River (latitude: 46.547413° and longitude: −118.177632°), Lower Snake River (latitude: 46.598604° and longitude: −118.234640°) and Columbia River (latitude: 46.231026° and longitude: −119.191049°). Vessels containing eggs or milt were placed on ice and together with the water were transferred to the hatchery at the Northwest Fisheries Science Center (NWFSC), Seattle, WA. Water collected from these three rivers, plus approximately 130 L of water from NWFSC hatchery, was stored separately and used as the four treatments in our experiment (see below). NWFSC hatchery water was dechlorinated water from the city of Seattle, WA, and was recirculated and filtered with UV light and biofiltration.

At the NWFSC, eggs and milt from all adults were mixed for several minutes, and fertilised eggs were disinfected in an iodine solution (50 mg/L) for 30 min following procedures outlined by U.S. Fish and Wildlife Service (1995). Approximately 250 fertilised eggs were randomly selected and transferred into each of four replicate emergence chambers within each of our four water treatments (Figure 1a). Emergence chambers were built of PVC (12.7 cm diameter) following

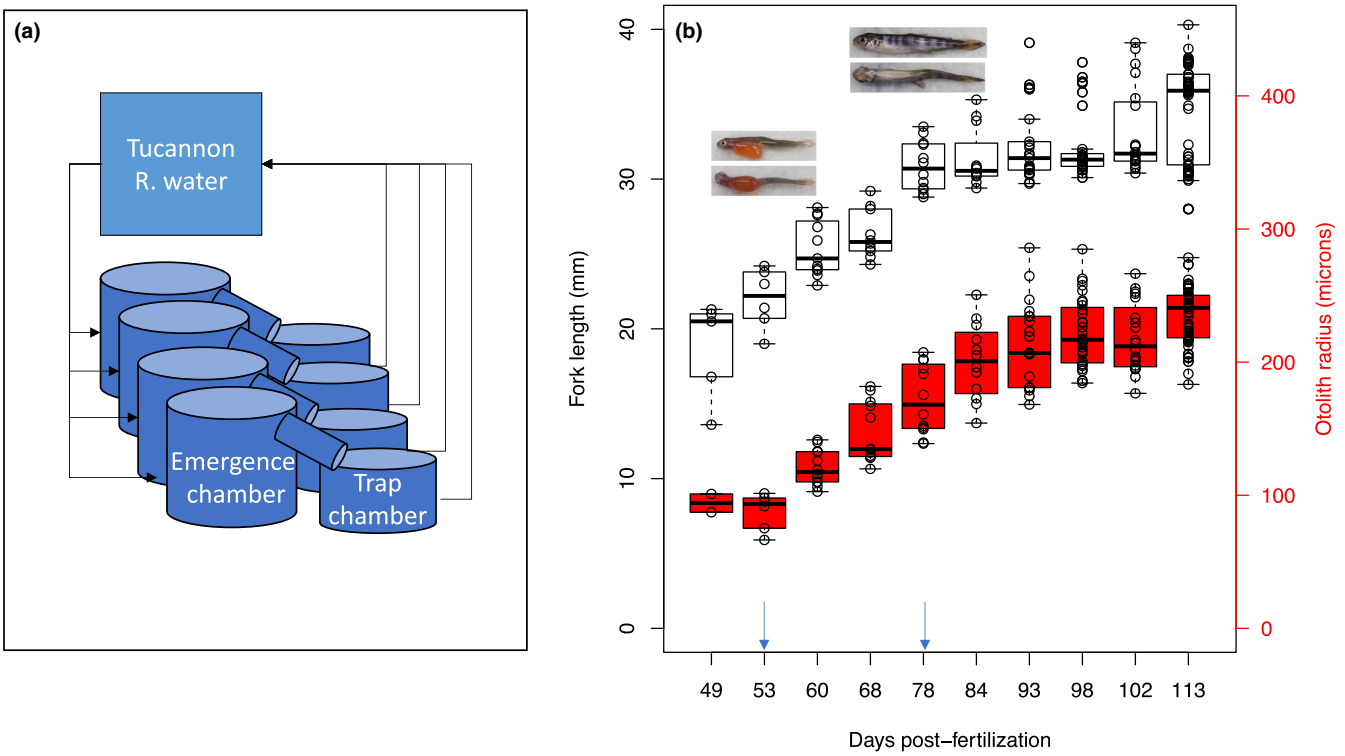

FIGURE 1 (a) Representation of the experimental setup for a treatment. Arrows show the direction of water flow from the Tucannon River holding container to emergence and trap chambers and then its return. (b) Boxplot of fork length (mm, black boxplot and left *y*-axis) and otolith radius (μm, red boxplot and right *y*-axis), pooled across treatments, with respect to days postfertilisation. Each circle corresponds to an individual, and we collected 3–15 fry from each treatment every 4–10 days starting at day 49 and ending on day 113. Arrows at days 53 and 78 indicate when 100% of the surviving eggs hatched and when the yolk sac was absorbed respectively. Inset pictures of lateral and ventral views of Chinook salmon (taken by A. Fuhrman) indicate the degree of yolk present at approximately days 53 and 78

the design used by (Steel et al., 2012). We filled each emergence chamber with 20 biofilter media (bio balls with a diameter of 20 mm) on top of which we poured our fertilised eggs. At the top of each emergence, chamber was an opening that permitted hatched fry to move into an adjacent trap chamber also built of PVC (7.6 cm diameter). Water drained from each of the four trap chambers via a mesh-covered outlet into a treatment-specific trough. An aquarium pump was used to pump water from the treatment-specific trough to each of the four replicate emergence chambers.

The experiment began on November 21, 2017, when fertilised eggs were placed in the emergence chambers, and continued for 113 days until March 2, 2018. During the experiment, emergence and trap chambers were inspected daily and dead eggs and fish were removed. Early in the experiment (day 12), the Columbia River treatment was unintentionally diluted with NWFSC hatchery water and on day 13 the water in this treatment was replaced with water collected from Lake Washington (latitude: 47.644600° and longitude: −122.307822°) (Table 1). This Lake Washington water was used as an emergency source of water for this treatment until day 88 of the experiment, at which point we replaced it with newly collected Columbia River water. We chose to refill this treatment with Columbia River water, instead of continuing to use Lake Washington water, because the strontium isotope ratio for the former is substantially different from both Tucannon and Lower Snake Rivers. We refer to this treatment as the Columbia River/Lake Washington treatment. On day 88, we also replaced the water in Tucannon River and Lower Snake River treatments with newly collected water from Tucannon River and Lower Snake River, respectively, while the water in the NWFSC treatment was replaced with NWFSC hatchery water. Lastly, on day 94 we replaced the water in all treatments with water from their respective sources.

Over the course of the experiment, average temperature, across treatments, was 10.7°C (ranged between 7.1 and 14.1°C). We did not design our experiment to mimic temperatures that might be found either in the free-flowing river or in the hatchery. Fish were reared according to standard hatchery protocols (Stickney, 1991).

We collected 3–15 fry from each treatment every 4–10 days starting at day 49 (i.e., January 8, 2018) (Table 1). Fish were euthanized using MS-222 (Argent Chemical Laboratories, Redmond, WA[1]) and placed in a freezer at the NWFSC. At day 53, 100% of the surviving eggs hatched, and by day 78, we observed complete yolk sac absorption across treatments. Complete yolk sac absorption was defined as the lack of yolk sac visible upon inspection of the ventral portion of a fish's abdomen. On day 84, we transferred all surviving fish from their emergence and trap chambers into their treatment-specific troughs, removed the pumps, added an aerator and initiated daily feeding (BioVita Fry, Bio-Oregon, Longview, WA). Water quality soon deteriorated across treatments because of excretion and

TABLE 1 Number of otoliths processed per treatment and day of the experiment along with when water samples were collected for $^{87}Sr/^{86}Sr$ analysis (indicated as a "W")

	Treatments				
Day #	Tucannon River	L. Snake River	NWFSC	Columbia River/L. Washington	Changes to treatments
12	0	0	0	0	Columbia R. treatment partially filled with NWFSC water
13	0	0	0	0	Columbia R. water replaced with L. Washington water
15	0 (W)	0 (W)	0 (W)	0 (W)	
44	0 (W)	0 (W)	0 (W)	0 (W)	
49	1	0	1	0	
53	2	2	0	2	
60	3	3	3	3	
68	3	3	3	3	
78	3	3	3	3	
84	3	3	3	3	
88	0	0	0	0	Water replaced in all treatments; L. Washington water replaced with Columbia R. water
93	5	4	6	5	
94	0	0	0	0	Water replaced in all treatments
98	10	7	7	8	
102[a]	5 (W)	5 (W)	5 (W)	5 (W)	
113[a]	12[b] (W)	14[b] (W)	14[b] (W)	12[b] (W)	

Note: Treatment-related changes to water are also indicated.

Abbreviation: NWFSC, Northwest Fisheries Science Center.

[a]Water samples between days 102 and 113 were pooled within a treatment for $^{87}Sr/^{86}Sr$ analysis.

[b]$^{87}Sr/^{86}Sr$ and Sr/Ca were analysed for these otoliths.

undigested food despite daily removal of this material using aquarium nets. Therefore, on day 88, and again on day 94, we exchanged the water within each treatment with treatment-appropriate freshwater (Table 1). Lastly, for the purpose of evaluating how water $^{87}Sr/^{86}Sr$ changed through time within each treatment, we analysed 20 ml of water collected from each treatment at days 15, 44, 102 and 113.

2.2 | Otolith analyses

We measured fork length (mm), removed otoliths (Table 1) from collected fish and prepared otoliths using methods described by Chittaro et al. (2020). Specifically, left sagittal otoliths were mounted on glass microscope slides using thermoplastic cement (Crystal Bond, http://www.crystalbond.com). Each otolith was polished on both sides in a sagittal plane using slurries (600-grit silicon carbide, 5.0 aluminium oxide and 1.0 micropolish; http://www.buehler.com) and a grinding wheel with Buehler© 1500 micropolishing pads. Polishing ceased when the core was visible. We photographed polished otoliths using a digital camera (Leica DFC450) mounted on a compound microscope (Zeiss©) and measured otolith radius using Image Pro software (version 7.0; MediaCybernetics©). Otolith radius was measured along a transect perpendicular to the longitudinal axis on the dorsal side of the otolith. Along the same transect, we also measured otolith radius to the hatch and exogenous feeding checks, which are identified by a prominent dark band and are formed during the transition from embryo to fry and following yolk sac depletion respectively (Barnett-Johnson et al., 2007; Zhang et al., 1995).

We chemically analysed 12–14 fish per treatment that were collected on day 113. These polished otoliths were simultaneously analysed for $^{87}Sr/^{86}Sr$ and Sr/Ca at the Radiogenic Isotope and Geochronology Laboratory at Washington State University (Pullman, WA, USA) using a novel laser ablation split-stream method. Specifically, the surface of each otolith was ablated using a Teledyne 193 nm ArF laser, and the ablated material was divided and introduced, with helium as the carrier gas, to two independent mass spectrometers: ThermoFisher Neptune Plus multicollector inductively

coupled plasma mass spectrometer (MC-ICPMS) and ThermoFisher Element2 sector-field (ICPMS) for determining $^{87}Sr/^{86}Sr$ and Sr/Ca respectively. Further details about the split-stream configuration can be found in Hegg et al. (2020) and Hegg et al. (2021). The laser ablation sampling system was operated at a frequency of 20 Hz, a 35 μm spot size, and the laser beam moved at a speed of 10 μm/s using an automated microscope stage. The laser ablated the polished otolith along a transect from the otolith edge to its core (the transect was perpendicular to the longitudinal axis on the dorsal side of the otolith). This edge-to-core scan line on the otolith corresponds to the entire life of the fish.

Data acquisition during the LA-MC-ICPMS/LA-ICPMS analysis lasted 50 s, 14 s of which were designated for instrument calibration and gas background counts prior to the start of each ablation. Data were recorded with a 0.262 s integration time. Measurement of the ratio of ^{87}Sr and ^{86}Sr was calculated and corrected through simultaneous measurement of ^{83}Kr, ^{84}Sr, ^{85}Rb and ^{88}Sr and followed procedures outlined in Chittaro et al. (2019). Specifically, measurements were mass-bias corrected and corrected for interferences in ^{86}Kr, ^{87}Rb and Ca dimers using natural ratios, similar to Barnett-Johnson et al. (2005). To evaluate measurement accuracy, we analysed a marine shell standard that was assumed to be in equilibrium with the global seawater value of $^{87}Sr/^{86}Sr$ = 0.70918 (Faure & Mensing, 2004). The marine shell standard was analysed 3–4 times every 15–20 otolith samples. During the course of this study, the average $^{87}Sr/^{86}Sr$ value for the marine shell was 0.70919 (*SD* = 0.00004, *n* = 14). Values of otolith $^{87}Sr/^{86}Sr$ were adjusted using a correction factor calculated each analysis day from the average deviation of the shell standard to the marine value (Hegg, Kennedy, & Fremier, 2013). LA-ICPMS measured ^{88}Sr was normalised to the National Institute of Standards and Technology (NIST-610) standard, which was analysed at the beginning and end of each set of 15–20 otoliths. Calcium was used as an internal standard and strontium was reported as a ratio to calcium. $^{87}Sr/^{86}Sr$ and Sr/Ca data were reduced using a customised data reduction scheme (available from the seventh author; Fisher et al., 2017) written for the Iolite software platform (Paton et al., 2011).

2.3 | Water analyses

Water $^{87}Sr/^{86}Sr$ was analysed using an Isotopx Phoenix thermal ionisation mass spectrometer (TIMS) at the Kennedy Laboratory of Integrated Fish Ecology, University of Idaho. Water samples were dried and prepared in a positive pressure particulate clean room under a HEPA filtered laminar flow hood. After drying, water samples were acidified and loaded in Savillex Teflon™ microcolumns containing approximately 0.21 ml strontium resin (i.e., Eichron Sr Spec ion exchange resin; 100–150 μm) to separate Sr and eluted first with 0.5 ml 8N HNO_3 and then 2.8 ml 3N HNO_3. Resin-bound strontium was then collected with 2 ml of 0.05 ml HNO_3 in clean Teflon™ vials.

Baseline samples were run between data blocks to correct for any within-analysis noise on the detectors and analytical blanks were run every 3–4 samples to ensure that no detectable Sr was measured on the tantalum filament with activator gel and phosphoric acid. Lastly, procedural blanks are periodically prepared using the same Sr-specific resin and elution scheme to ensure that lab materials contain no background Sr. We analysed water samples collected on days 15 and 44, and due to limited sample volume, we pooled water collected on days 102 and 113 (Table 1). Throughout the analyses of water samples, a replicate analysis of the National Institute of Standards and Technology standard reference material (SRM-987) yielded mean $^{87}Sr/^{86}Sr$ of 0.710248 (*SD* = 0.000004, *n* = 11).

2.4 | Statistical analyses

To assess if growing conditions varied among treatments we used an analysis of variance (ANOVA) to test whether fork length and otolith radius differed among treatments for fish collected at the end of the experiment (i.e., day 113). Next, we evaluated the extent to which otolith core $^{87}Sr/^{86}Sr$ and Sr/Ca varied among treatments using the Kruskal-Wallis one-way analysis of variance. The otolith core $^{87}Sr/^{86}Sr$ and Sr/Ca were defined as the average from the core to a radius of 25, 50, 75, 100 and 125 μm. We did not expect a significant difference in otolith core $^{87}Sr/^{86}Sr$ and Sr/Ca among treatments, particularly for the smaller radii, since the otolith values would be maternally derived and the product of the same females whose fertilised eggs were randomly distributed among treatments.

To identify the otolith radius corresponding to a shift in $^{87}Sr/^{86}Sr$ and Sr/Ca we treated each edge-to-core transect of $^{87}Sr/^{86}Sr$ and Sr/Ca as a separate timeseries and performed change-point analysis on each. A change-point is an instance in time where the statistical properties before and after this time point differ (Killick & Eckley, 2014). We used the change-point package available for R (R Core Team, 2021) from the Comprehensive R Archive Network (CRAN) at http://CRAN.R-project.org/ package = change-point (Killick & Eckley, 2014).

The change-point analysis uses a likelihood ratio-based approach to test the hypothesis of no change-point (null) and a change-point (alternative). If a change-point is detected (i.e., null hypothesis is rejected) its position in the timeseries was then estimated (Killick & Eckley, 2014). Our analysis focused on identifying a shift in mean $^{87}Sr/^{86}Sr$ and Sr/Ca for each individual and then determining the otolith radius at which this shift occurred.

For all edge-to-core transects of $^{87}Sr/^{86}Sr$ and Sr/Ca we used a binary segmentation algorithm (method = "BinSeg") included within the change-point package, which first applies a single change-point test statistic to the timeseries data. If a change-point is identified the data are divided into two at the change-point location. The change-point procedure is then repeated on the two new data sets, before and after the first identified change-point, and the process continues until no additional change-points are found or if an insufficient amount of data is available within a segment to evaluate if a change-point is present.

We set the maximum number of change-points to 15 ($Q = 15$) for $^{87}Sr/^{86}Sr$ and Sr/Ca data of fish from all treatments, except L. Snake River (see below). Fifteen was chosen because it was the maximum number of possible change-points, given the length of $^{87}Sr/^{86}Sr$ and Sr/Ca data for our smallest otolith and the number of segments that could be accommodated between change points. Because the first change-point to be identified represents the largest shift in mean $^{87}Sr/^{86}Sr$ and Sr/Ca values within a timeseries, we assumed that this change-point corresponded to the transition from maternally to environmentally derived $^{87}Sr/^{86}Sr$ and Sr/Ca in an otolith. Finally, we excluded the L. Snake River treatment from the change-point analysis of $^{87}Sr/^{86}Sr$ data because $^{87}Sr/^{86}Sr$ levels in the otolith and water were expected to be similar as a result of residence of the adult females from which eggs were extracted.

We evaluated the extent to which otolith radius at the first change-point varied among treatments, separately for $^{87}Sr/^{86}Sr$ and Sr/Ca data, using Kruskal-Wallis one-way analysis of variance. To estimate fish age and fork length at change-point, we used the average otolith radius at the first change-point together with relationships we generated between days postfertilisation and otolith radius, and fork length and otolith radius respectively.

To estimate the portion of the otolith representing natal origin, we identified the otolith radius that corresponded to when otolith $^{87}Sr/^{86}Sr$ converged with water $^{87}Sr/^{86}Sr$ of the treatment in which the fish resided. We defined this convergence as the otolith radius of the core-to-edge transect in which the otolith $^{87}Sr/^{86}Sr$ was relatively similar (i.e., within +/−0.00075) to that of water $^{87}Sr/^{86}Sr$ and remains within this range to the edge of the otolith. The water $^{87}Sr/^{86}Sr$ used as the basis for assessing this convergence was collected on days 102 and 113 for the NWFSC and Columbia R./Lake Washington treatments, while day 44 was used for the Tucannon R. treatment since we did not have sufficient water collected on days 102 and 113 (see Results) to yield water $^{87}Sr/^{86}Sr$. We assumed that the water $^{87}Sr/^{86}Sr$ from day 44 was similar to that from day 102 and 113 given the stability in water $^{87}Sr/^{86}Sr$ observed in the L. Snake River and NWFSC treatments (see Results). L. Snake River was excluded from this analysis because the $^{87}Sr/^{86}Sr$ levels in the otolith and water were expected to be similar as a result of the residence of the adult females from which eggs were extracted. Although studies have indicated a 1:1 relationship between water $^{87}Sr/^{86}Sr$ and otolith $^{87}Sr/^{86}Sr$ (Kennedy et al., 2000) we did not expect otolith $^{87}Sr/^{86}Sr$ to match that of the water in which the fish resided in our study because of the dietary contribution of a marine-based feed to otolith $^{87}Sr/^{86}Sr$ that would have a marine $^{87}Sr/^{86}Sr$ signature (Janak et al., 2021; Kennedy et al., 2000).

3 | RESULTS

Visual observation of fish among treatments indicated that surviving eggs hatched no later than day 53 of the experiment and yolk sac absorption occurred no later than day 78 (mean fork length of 22 and 30 mm respectively). Fork length and otolith radius ranged from 13 to 40 mm and 64 to 315 μm, respectively, for fish collected throughout the experiment (Figure 1b). ANOVA's did not reveal significant differences among treatments in terms of body size nor otolith radius for fish collected at day 113 of the experiment. Of 52 fish collected at day 113, we identified hatch and exogenous feeding checks for 49 and 40 individuals respectively (Table S1). We had difficulty discerning the exogenous feeding check for nine individuals, which may be a result of this check being less prominent in hatchery fish as reported by Barnett-Johnson et al. (2007). For the remaining three individuals, we had difficulty discerning the hatch and exogenous feeding checks because of poor image quality.

TABLE 2 Water $^{87}Sr/^{86}Sr$ values (and standard error) per treatment and day of experiment

Treatment	Day of experiment	$^{87}Sr/^{86}Sr$	±2*SE*
Tucannon River	15	0.707236	0.000004
Tucannon River	44	0.707329	0.00001
Tucannon River	102 and 113	–	–
Lower Snake River	15	0.709611	0.000004
Lower Snake River	44	0.709447	0.000004
Lower Snake River	102 and 113	0.709648	0.00001
NWFSC	15	0.707571	0.000004
NWFSC	44	0.707567	0.000004
NWFSC	102 and 113	0.707523	0.000004
Columbia R./Lake Washington	15	0.706751	0.000004
Columbia R./Lake Washington	44	0.706917	0.000004
Columbia R./Lake Washington	102 and 113	0.711791	0.000004

Note: Insufficient water was available for analysis for the Tucannon River treatment on days 102 and 113.

Water $^{87}Sr/^{86}Sr$ ratios were relatively stable across the three sampling events within each treatment except for Columbia River/Lake Washington, which showed a change we attributed to the addition of water from Lake Washington (Table 1). Specifically, water $^{87}Sr/^{86}Sr$ went from 0.7067 at day 15 and 0.7069 at day 44 to 0.7117 at days 102 and 113 (Table 2). Our water $^{87}Sr/^{86}Sr$ from the Columbia River/Lake Washington treatment collected on days 102 and 113 was lower than Columbia River water reported by other studies (0.713–0.717; Janak et al., 2021, Miller et al., 2011). We suspect that our lower value was due to a residual amount of Lake Washington water that resulted in a diluted Columbia River/Lake Washington water $^{87}Sr/^{86}Sr$. We did not report water $^{87}Sr/^{86}Sr$ for days 102 and 113 from Tucannon River because we had an insufficient amount of water for analysis. Lastly, our Kruskal-Wallis test comparing otolith core $^{87}Sr/^{86}Sr$ among treatments indicated nonsignificant differences at otolith radii of 25, 50 and 75, but significant differences at 100 (K-W chi-squared = 13.7, $df = 3$ and p-value < .01) and 125 μm (K-W chi-squared = 20.4, $df = 3$ and p-value < .001), while the same

analysis for otolith core Sr/Ca did not show significant differences among treatments for any otolith radius.

3.1 | Change-point analysis

Otolith $^{87}Sr/^{86}Sr$ ratios trended towards water $^{87}Sr/^{86}Sr$ values within each treatment and otolith Sr/Ca values decreased with increasing distance from the core (Figure 2). Multiple change-points were identified for each fish, and with the exception of the first identified change-point, we assumed them, for the purpose of this study, to be uninformative and not necessarily associated with an actual change in the fish's exposure to relevant elements (Figures 3 and S1–S8).

Fish that reared within the Tucannon River treatment ($n = 12$) had otolith $^{87}Sr/^{86}Sr$ that trended towards the average water $^{87}Sr/^{86}Sr$ of 0.7072 (Table 2, Figure 2a). According to change-point analysis, a shift in $^{87}Sr/^{86}Sr$ and Sr/Ca (i.e., the first identified change-point)

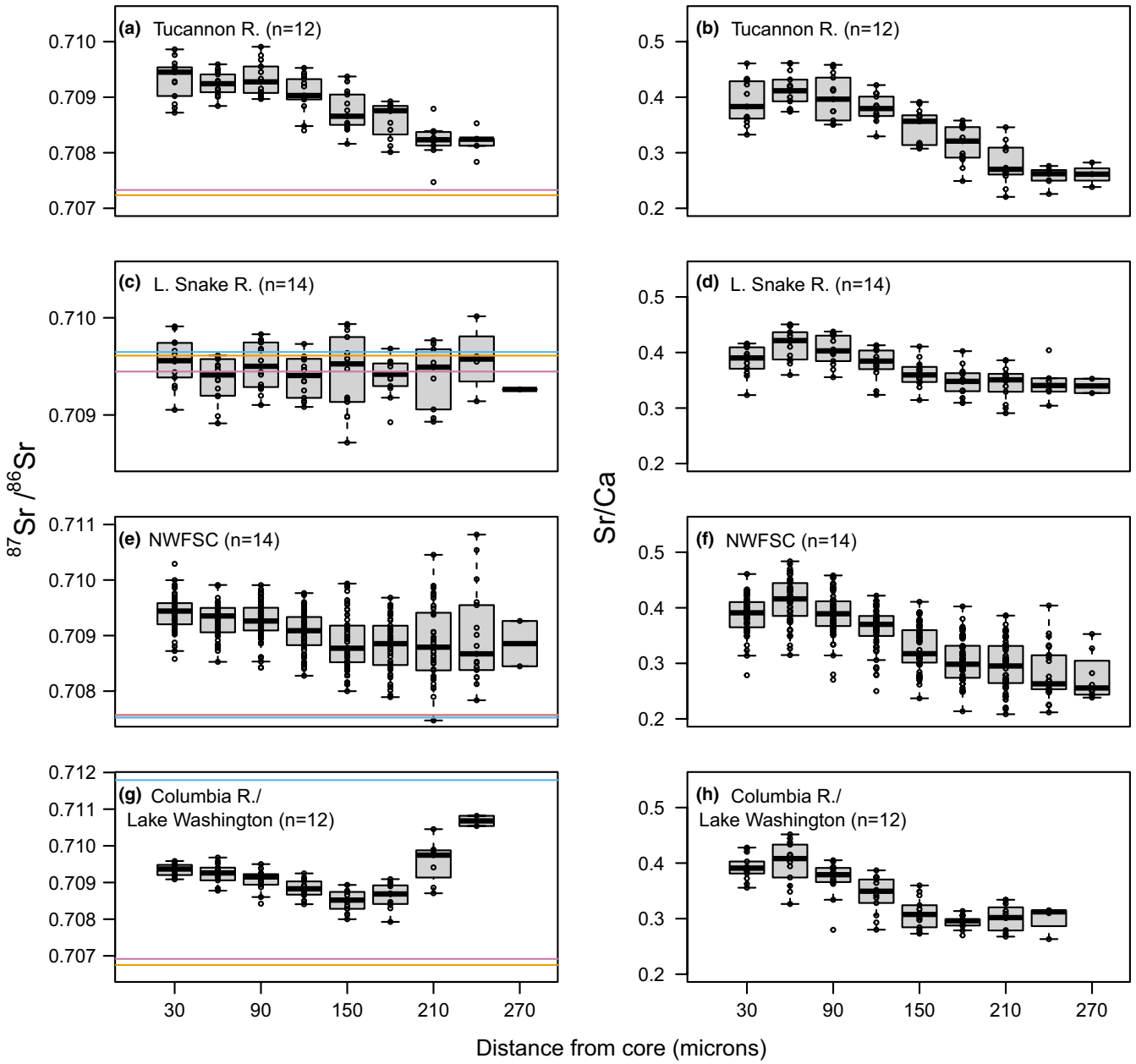

FIGURE 2 Boxplots of otolith $^{87}Sr/^{86}Sr$ and Sr/Ca with respect to sections (~30 μm) of the edge-to-core transect for each individual and averaged across individuals within a treatment: (a and b) Tucannon River, (c and d) Lower Snake River, (e and f) NWFSC hatchery and (g and h) Columbia River/Lake Washington. Median, the 25th and 75th percentile, and range are represented by thick horizontal line, top and bottom of box, and whiskers respectively. Black dots correspond to individual $^{87}Sr/^{86}Sr$ and Sr/Ca data. Water $^{87}Sr/^{86}Sr$ values are represented as the horizontal orange (day 15 of the experiment), purple (day 44) and blue (pooled days 102 and 113) lines. The blue line is absent from Tucannon River (plot a) because insufficient water was available for analysis. For NWFSC (e), the three lines are difficult to visually discern due to the similarity in water $^{87}Sr/^{86}Sr$ values (see Table 2). *Y*-axes differ among plots of $^{87}Sr/^{86}Sr$ values

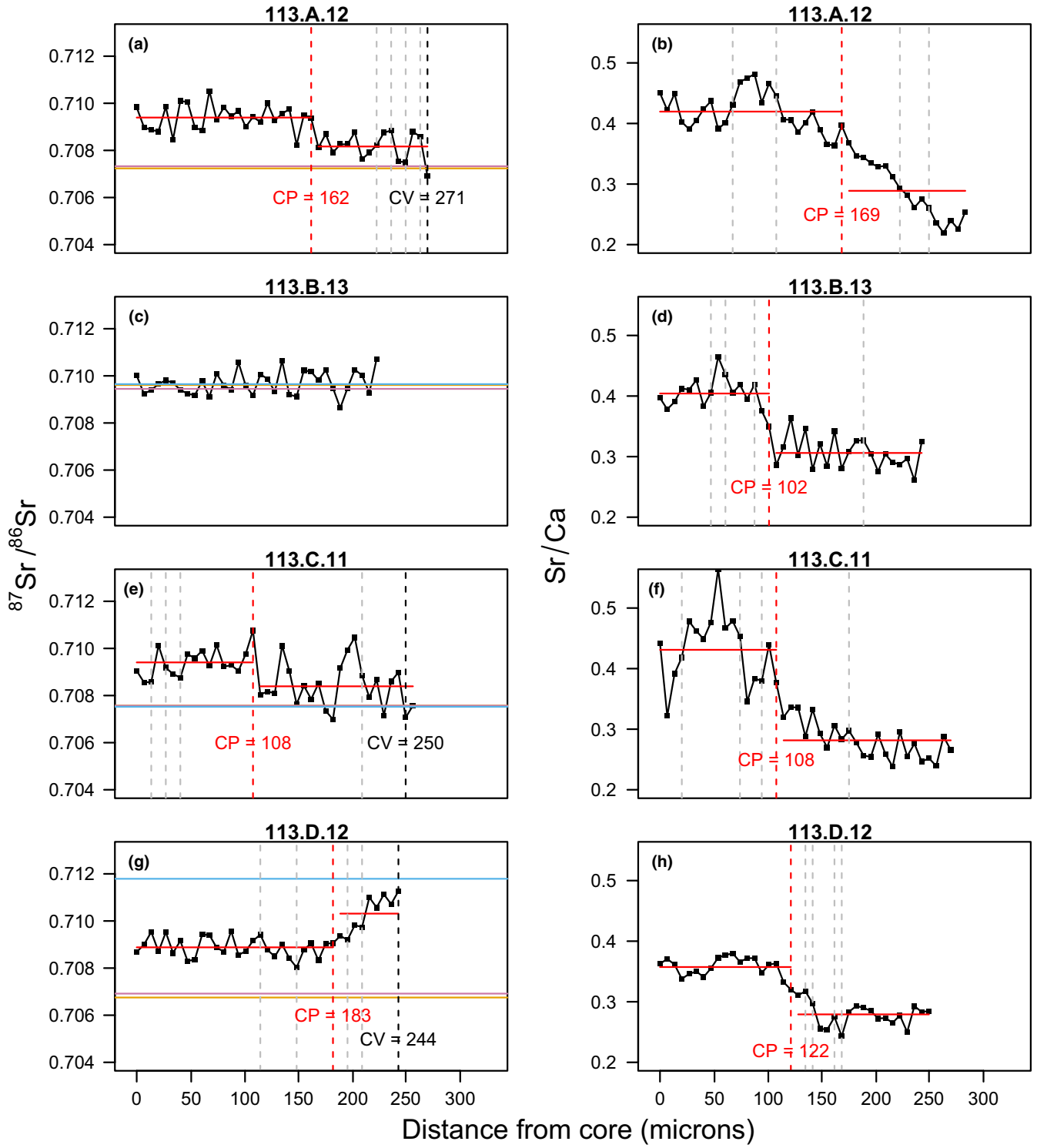

FIGURE 3 Plots of otolith $^{87}Sr/^{86}Sr$ and Sr/Ca with respect to distance from otolith core (μm) for one representative fish from each treatment: (a and b) Tucannon River (fish 113.A.12), (c and d) Lower Snake River (fish 113.B.13), (e and f) NWFSC hatchery (fish 113.C.11) and (g and h) Columbia River/Lake Washington (fish 113.D.12). Red horizontal lines correspond to the portions of the otolith before and after the first identified change-point (CP; red vertical line), and grey vertical lines indicate the otolith radius of four subsequent change-points. To improve visual clarity, only the first five change-points are displayed. Water $^{87}Sr/^{86}Sr$ values are represented as the horizontal orange (day 15 of the experiment), purple (day 44) and blue (pooled days 102 and 113) lines. The blue line is absent from Tucannon River (plot a) because insufficient water was available for analysis. For NWFSC (plot e), three lines are difficult to visually discern due to the similarity in water $^{87}Sr/^{86}Sr$ values (Table 2). Vertical black line corresponds to the otolith radius at which otolith and water $^{87}Sr/^{86}Sr$ values converged (CV). We defined this convergence as the otolith radius of the core-to-edge transect in which the otolith $^{87}Sr/^{86}Sr$ was relatively similar (i.e., within +/−0.00075) to that of water $^{87}Sr/^{86}Sr$ and remains within this range to the edge of the otolith. Estimates of otolith radius at convergence were not calculated for fish from the Lower Snake River treatment because their $^{87}Sr/^{86}Sr$ levels in the otolith and water were expected to be similar for the entire core-to-edge transect

occurred at an average otolith radius of 147 and 143 μm respectively (Figures 3a,b, S1 and S2, and Table 1). Otolith $^{87}Sr/^{86}Sr$ before and after the first change-point averaged 0.7092 (0.0002 standard deviation) and 0.7082 (0.0002 standard deviation) respectively. Otolith Sr/Ca before and after the first change-point averaged 0.3925 (0.019 standard deviation) and 0.2845 (0.01 standard deviation) respectively.

Fish that reared within the Lower Snake River treatment ($n = 14$) had otolith $^{87}Sr/^{86}Sr$ that remained aligned with the average water value of 0.7095 (Table 2, Figures 2c and S3). According to change-point analysis, a shift in Sr/Ca occurred at an average otolith radius of 126 μm (Figures 3d, S4 and Table 1). Otolith Sr/Ca before and after this first identified change-point averaged 0.3999 (0.011 standard deviation) and 0.3448 (0.02 standard deviation) respectively.

Fish that reared within the NWFSC treatment ($n = 14$) had otolith $^{87}Sr/^{86}Sr$ that trended towards the average water $^{87}Sr/^{86}Sr$ of 0.70755 (Table 2, Figure 2e). According to change-point analysis, a shift in $^{87}Sr/^{86}Sr$ and Sr/Ca occurred at an average otolith radius of 108 and 123 μm respectively (Figures 3e,f, S5 and S6, and Table 1). Otolith $^{87}Sr/^{86}Sr$ before and after the first identified change-point averaged 0.7094 (0.0002 standard deviation) and 0.7086 (0.0001 standard deviation) respectively. Otolith Sr/Ca before and after the first identified change-point averaged 0.3877 (0.0362 standard deviation) and 0.2612 (0.0126 standard deviation) respectively.

Fish that reared within the Columbia River/Lake Washington treatment ($n = 12$) had otolith $^{87}Sr/^{86}Sr$ that trended first towards the average water $^{87}Sr/^{86}Sr$ of 0.7068 from days 15 and 44 and then towards water $^{87}Sr/^{86}Sr$ of 0.7117 from days 102/113 (Table 2, Figure 2g). According to change-point analysis, a shift in $^{87}Sr/^{86}Sr$ and Sr/Ca occurred at an average otolith radius of 143 and 113 μm respectively (Figures 3g,h, S7 and S8, and Table 1). Otolith $^{87}Sr/^{86}Sr$ before and after the first identified change-point averaged 0.7091 (0.0003 standard deviation) and 0.7102 (0.0007 standard deviation) respectively. Otolith Sr/Ca before and after the first identified change-point averaged 0.3851 (0.0223 standard deviation) and 0.3011(0.0156 standard deviation) respectively.

Otolith radius at the first identified change-point did not differ significantly among treatments for otolith $^{87}Sr/^{86}Sr$ and Sr/Ca data (Figure 4). Across treatments, our results indicated a shift in $^{87}Sr/^{86}Sr$ and Sr/Ca occurred, on average, at 132 μm (±50 μm standard deviation) and 127 μm (±29 μm), respectively, from the otolith core. We estimated that the shift in otolith $^{87}Sr/^{86}Sr$ occurred at day 70 postfertilisation and at a fork length of 26 mm when using the average otolith radius at the first identified change-point together with the relationships we generated between days postfertilisation and otolith radius and between fork length and otolith radius (Figure S9a,b). Further, the otolith radius at the first identified change-point for $^{87}Sr/^{86}Sr$ and Sr/Ca was, on average, 69 and

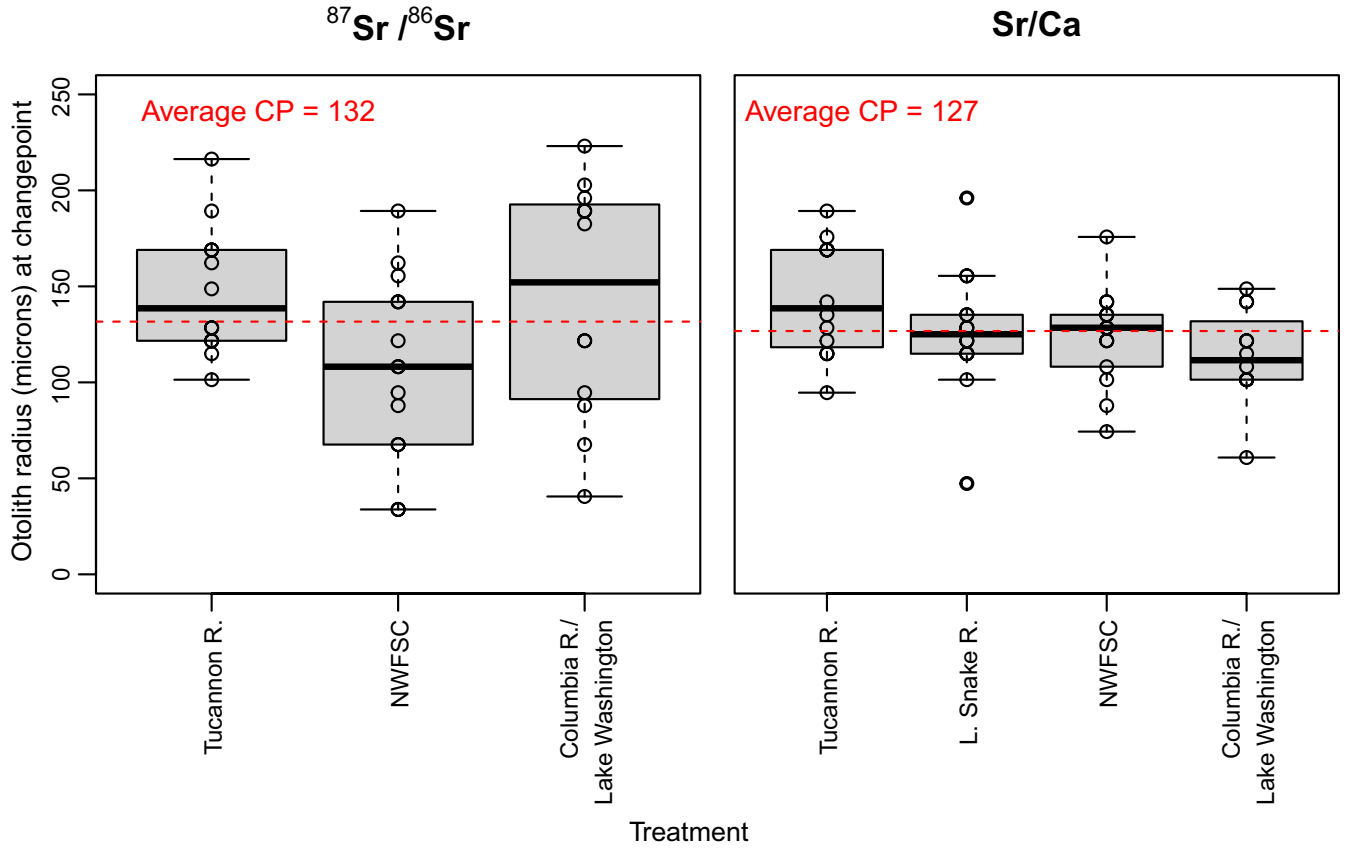

FIGURE 4 Boxplot of otolith radius at the first identified change-point in $^{87}Sr/^{86}Sr$ and Sr/Ca for each treatment. Each circle represents an individual. The red horizontal line indicates the mean otolith radius at change-point (CP) across treatments for $^{87}Sr/^{86}Sr$ (132 μm; ±50 μm standard deviation) and Sr/Ca (127 μm; ±29 μm)

74 μm less, respectively, than the otolith radius to the exogenous feeding check (average 202 μm and standard deviation 19.5 μm; Table S1).

By the end of the 113-day experiment, approximately 39% (i.e., 15 of 38) of the analysed otoliths had $^{87}Sr/^{86}Sr$ that converged with that of their water treatment (Figures 3, S1, S5 and S7). For these 15 fish, otolith radius was estimated to be, on average, 244 μm (±23 μm standard deviation), which corresponded to day 106 postfertilisation and a 34 mm fork length, when using the average otolith radius at convergence together with the mathematical relationships we generated between days postfertilisation and otolith radius and between fork length and otolith radius (Figure S9a,b). We did not include fish from the Lower Snake River treatment (n = 14) in this analysis because their otolith $^{87}Sr/^{86}Sr$ overlapped with that of their treatment water for the entire otolith core-to-edge transect. This lifetime equilibrium for fish from the Lower Snake River treatment was likely due to the fact that the adult females used in this experiment resided in Snake River prior to collection and incorporated and transferred the $^{87}Sr/^{86}Sr$ from the river into their developing eggs.

4 | DISCUSSION

Identifying the natal origin of fish is often necessary for effective species management and conservation. In this study, we sought to identify the portion of the otolith formed during an early developmental stage, representing the transition to environmentally derived strontium isotopes, so as to accurately investigate questions of natal origin for a threatened population of fall Chinook salmon (*Oncorhynchus tshawytscha*). Our results indicated that the transition from maternally to the environmentally derived source of $^{87}Sr/^{86}Sr$ and Sr/Ca occurred, on average, at an otolith radius of 132 and 127 μm, respectively, which corresponded to the developmental time between hatching and exogenous feeding.

4.1 | Stability of otolith core $^{87}Sr/^{86}Sr$ and Sr/ca

Our findings of nonsignificant differences in $^{87}Sr/^{86}Sr$ among treatments, with respect to an otolith radius of ≤75 μm, were not surprising given that the fish used in this experiment were the offspring of two adult females, both of which were collected after migrating through the same river (i.e., Lower Snake River). This similarity in otolith core $^{87}Sr/^{86}Sr$ for otolith radius of ≤75 μm, despite the development of fish within treatments that differed with respect to water $^{87}Sr/^{86}Sr$ (Table 2), supports the notion of the egg being a chemically closed system prior to and at this stage of development. The limited exchange between the environment and the growing otolith was further supported by the elevated otolith Sr/Ca levels in the core region (≤90 μm; Figure 2) that are likely the product of maternal marine residency. The fact that the otolith Sr/Ca levels did not differ significantly among treatments was also not surprising given that salinity, which is known to be positively related to otolith Sr/Ca levels (Zimmerman, 2005), was expected to be uniform among our freshwater treatments.

Our otolith $^{87}Sr/^{86}Sr$ data suggested that, in general, this portion of the otolith core (i.e., an otolith radius ≤75 μm) is a good marker of maternal contribution and thus can be used to indicate maternal anadromy (Courter et al., 2013). However, research has shown that the effectiveness of using the otolith core as an indicator of maternal anadromy declines with longer freshwater migration (Donohoe et al., 2008; Miller & Kent, 2009). For example, studies have shown that an anadromous isotope signal was detected in the core of otoliths from juvenile Chinook salmon that hatched in close proximity to the ocean (i.e., <200 km), yet no signal was observed for individuals sampled over 1000 km inland (Bacon et al., 2004). In fact, Hegg et al. (2018) reported that for females with a substantial freshwater migration, the egg $^{87}Sr/^{86}Sr$ could shift up to 0.00086 within the first 80 h after being laid and as much as 0.00091 at hatching. Their findings therefore conflict with the idea that the egg is a chemically closed system and caution against the use of the otolith core as a marker of maternal anadromy for certain species. It should be noted that eight individuals in our study showed shifts in otolith $^{87}Sr/^{86}Sr$ or Sr/Ca at an otolith radius less than 75 μm (e.g., change-point analysis for fish #113.C.15 indicated the first identified change-point occurred at 67 and 74 μm, respectively; Figures 4 and S5). The shifts in $^{87}Sr/^{86}Sr$ or Sr/Ca for these eight fish occurred prior to hatching and thus challenge the notion of the egg being a chemically closed system at this developmental stage; an otolith radius of 75 μm was estimated to correspond to an age of 40 days postfertilisation (Figure S9a), which was approximately when we observed hatching start across treatments, while 83 μm was the average otolith radius at hatch check (Table S1).

4.2 | Environmentally derived $^{87}Sr/^{86}Sr$ and Sr/ca

The dissimilarity in otolith core $^{87}Sr/^{86}Sr$ among treatments, with respect to an otolith radius of ≥100 μm, suggested that treatment-specific strontium isotopes were being sequestered into the growing otoliths at this stage of larval development. In fact, fish reared in each of our four treatments showed otolith $^{87}Sr/^{86}Sr$ that shifted towards the water $^{87}Sr/^{86}Sr$ in which they resided (Figure 2).

According to the change-point analysis, a shift in the otolith $^{87}Sr/^{86}Sr$ and Sr/Ca occurred, on average, at an otolith radius of 132 μm and 127 μm, respectively, across treatments (Figure 4 and Table S1). We assumed this first identified the shift in otolith $^{87}Sr/^{86}Sr$ and Sr/Ca corresponded to the transition from a maternally to environmentally derived source of strontium. Our estimate of where this transition in otolith $^{87}Sr/^{86}Sr$ occurred, averaged across treatments, was similar to that of Hegg et al. (2018) who reported it at an otolith radius of approximately 150 μm and which they associated with hatching. In our study, we estimated that this average otolith $^{87}Sr/^{86}Sr$ shift likely occurred between hatching and exogenous feeding since the otolith radii for these two developmental stages were, on average, estimated to be 83

and 202 μm, respectively (Table S1); we also observed hatching and yolk sac absorption to have occurred no later than day 53 and 78, respectively, which corresponded to an estimated otolith radius of 93 and 177 μm respectively (Figure S9c). In contrast, Hegg et al. (2018) reported the shift occurred later, approximately 225 μm, with respect to otolith elemental signatures (i.e., Mn/Ca, Ba/Ca and Sr/Ca), and thus suggested that this transition represented an ontological change within the developing fish separate from hatching and possibly related to fish emergence. Interestingly, work on a related salmonid (*Oncorhynchus nerka*) by Janak et al. (2021) reported shifts in otolith $^{87}Sr/^{86}Sr$ and Sr/Ca associated with hatching and yolk sac absorption that occurred at an average otolith radius of 67 and 118 μm, respectively, which was comparable to this study.

Although we detected an environmentally derived source of $^{87}Sr/^{86}Sr$ in the otolith, the timing of which likely occurred between hatching and exogenous feeding, convergence between otolith and water $^{87}Sr/^{86}Sr$ was only observed in 39% of our otoliths (i.e., 15 of 38) by the end of the experiment at day 113 (Figures 3, S1, S5 and S7). These 15 fish had an otolith radius at convergence that ranged from 190 to 278 μm and the fact that this convergence occurred after exogenous feeding (Table S1) supports the assumption made by Barnett-Johnson et al. (2007, 2008) that this life stage is an important marker of the uptake of environmentally derived isotopes within the otolith. Hegg et al. (2018) reported otolith $^{87}Sr/^{86}Sr$ reaches a stable period at approximately 250 to 300 μm, which for the purposes of reconstructing natal origin, would ensure that the otolith $^{87}Sr/^{86}Sr$ attains equilibrium with that of the water in which the fish reared. Given that a substantial proportion of our otoliths did not show convergence between otolith and water $^{87}Sr/^{86}Sr$ in our experiment, which was likely due to the dietary contribution of marine-based feed, we are unable to recommend an otolith radius to target for the reconstructing natal origin apart from one that is greater than approximately 130 μm.

5 | CONCLUSION

The application of strontium isotopes in the otoliths of anadromous fishes, like salmonids, has been a powerful tool in understanding the extent to which different natal and rearing rivers to contribute individuals to the adult population (Brennan et al., 2015; Brennan & Schindler, 2017; Hegg, Kennedy, Chittaro, & Zabel, 2013; Kennedy et al., 1997). Complicating this work, however, is the fact that during an individual's larval stage, there is a shift in the source of strontium, from maternally to environmentally derived, that is deposited onto their growing otolith. The results of this experiment corroborate earlier work that indicated a period between hatching and exogenous feeding as an important point in larval development representing the transition from maternally to environmentally derived strontium isotopes in otoliths, and that the period following exogenous feeding likely corresponds to the equilibration of environmentally derived strontium isotope signature in otoliths.

As otolith studies of juvenile life history have increased in temporal and spatial resolution, it is increasingly important to understand this transition from maternal to juvenile chemistry in the early otolith record to avoid biasing natal origin determinations. It is also critical to exclude chemical signatures of the natal reach from studies of maternal anadromy. While Sr/Ca as a marker of maternal anadromy has been a staple of the otolith literature for some time (Kalish, 1990), the use of $^{87}Sr/^{86}Sr$ as a marker for maternal anadromy is relatively recent (Courter et al., 2013). Despite this, the mechanisms of when and how this isotopic change from maternal to natal sources of strontium occur in the developing fish have only recently been investigated (Hegg et al., 2018), and controlled experiments demonstrating these changes are lacking (Janak et al., 2021). This work provides experimental evidence of the transition from maternally to environmentally derived isotopic signatures in the developing otolith. These results confirm many of the circumstantial conclusions from the prior literature while providing evidence of the timing of this transition in $^{87}Sr/^{86}Sr$ and Sr/Ca in Chinook salmon and a template for future studies in other species.

AUTHOR CONTRIBUTIONS

Paul Chittaro, Jens Hegg, Abby Fuhrman and Brian Beckman conceived and designed the investigation. Paul Chittaro, Abby Fuhrman, Brian Beckman, Chris Fisher and Brian Kennedy performed field and/or laboratory work. Paul Chittaro, Jens Hegg, Devin Robichaux and Rothboury Doung analysed the data. Chris Fisher, Jeff Vervoort and Brian Kennedy contributed materials, reagents and/or analysis tools. Paul Chittaro and Jens Hegg wrote the paper.

ACKNOWLEDGEMENTS

Special thanks to K. Gillies-Rector (University of Idaho), R. Zabel (NWFSC), K. Tiffan (U.S. Geological Survey) and D. Milks (WDFW), who provided assistance with experimental design and setup, and to M. Bond and A. Luckenbach for their constructive comments. Milt and eggs were collected under WDFW Permit # 7616-09-06-17. Hollings undergraduate scholarship was awarded to D. Robichaux. This work was funded by grants from Bonneville Power Administration (#46273-REL-127). All applicable institutional and/or national guidelines for the care and use of animals were followed. We thank J. Janak and an anonymous reviewer for their helpful comments.

CONFLICT OF INTEREST

The authors declare that they have no conflict of interest.

DATA AVAILABILITY STATEMENT

The data that support the findings of this study are available from the corresponding author upon reasonable request.

ORCID

Paul Chittaro https://orcid.org/0000-0001-9310-7314
Jens Hegg https://orcid.org/0000-0003-0125-9287
Abby Fuhrman https://orcid.org/0000-0003-1050-2197

ENDNOTE

[1]Reference to trade names does not imply endorsement by the National Marine Fisheries Service, NOAA.

REFERENCES

Bacon, C. R., Weber, P. K., Larsen, K. A., Reisenbichler, R., Fitzpatrick, J. A., & Wooden, J. L. (2004). Migration and rearing histories of Chinook salmon (*Oncorhynchus tshawytscha*) determined by ion microprobe Sr isotope and Sr/ca transects of otoliths. *Canadian Journal of Fisheries and Aquatic Sciences*, *61*, 2425–2439.

Barnett-Johnson, R., Grimes, C., Royer, C., & Donohoe, C. (2007). Identifying the contribution of wild and hatchery Chinook salmon (*Oncorhynchus tshawytscha*) to the ocean fishery using otolith microstructure as natural tags. *Canadian Journal of Fisheries and Aquatic Sciences*, *64*, 1683–1692.

Barnett-Johnson, R., Pearson, T. E., Ramos, F. C., Grimes, C. B., & MacFarlane, R. B. (2008). Tracking natal origins of salmon using isotopes, otoliths, and landscape geology. *Limnology and Oceanography*, *53*, 1633–1642.

Barnett-Johnson, R., Ramos, F. C., Grimes, C. B., & MacFarlane, R. B. (2005). Validation of Sr isotopes in otoliths by laser ablation multicollector inductively coupled plasma mass spectrometry (LA-MC-ICPMS): Opening avenues in fisheries science applications. *Canadian Journal of Fisheries and Aquatic Sciences*, *62*, 2425–2430.

Brennan, S. R., & Schindler, D. E. (2017). Linking otolith microchemistry and dendritic isoscapes to map heterogeneous production of fish across river basins. *Ecological Applications*, *27*, 363–377.

Brennan, S. R., Zimmerman, C. E., Fernandez, D. P., Cerling, T. E., McPhee, M. V., & Wooller, M. J. (2015). Strontium isotopes delineate fine-scale natal origins and migration histories of Pacific salmon. Science. *Advances*, https://doi.org/10.1126/sciadv.1400124.

Brophy, D., Jeffries, T. E., & Danilowicz, B. S. (2004). Elevated manganese concentrations at the cores of clupeid otoliths: Possible environmental, physiological, or structural origins. *Marine Biology.*, *144*, 779–786.

Campana, S. E. (1992). Measurement and interpretation of the microstructure of fish otolith. In D. K. Stevenson & S. E. Campana (Eds.), *Otolith microstructure examination and analysis* (Vol. *117*, pp. 59–71). Canadian Special Publication of Fisheries and Aquatic Sciences.

Chittaro, P. M., Hegg, J. C., Kennedy, B. P., Weitkamp, L. A., Johnson, L. L., Bucher, C., & Zabel, R. W. (2019). Juvenile river residence and performance of Snake River fall Chinook salmon. *Ecology of Freshwater Fish*, *28*, 396–410.

Chittaro, P. M., Hogan, J., Gagnon, J., Fryer, B., & Sale, P. (2006). In situ experiment of ontogenetic variability in the otolith chemistry of *Stegastes partitus*. *Marine Biology*, *149*, 1227–1235.

Chittaro, P. M., Veggerby, K., Haught, K., & Sanderson, B. L. (2020). *Otolith processing and analysis*. NOAA Processed Report NMFS-NWFSC-PR-2020-02. p. 33. U.S. Department of Commerce.

Courter, I. I., Child, D. B., Hobbs, J. A., Garrison, T. M., Glessner, J. J. G., & Duery, S. (2013). Resident rainbow trout produce anadromous offspring in a large interior watershed. *Canadian Journal of Fisheries and Aquatic Sciences*, *70*, 701–710.

Donohoe, C., Adams, P., & Royer, C. (2008). Influence of water chemistry and migratory distance on ability to distinguish progeny of sympatric resident and anadromous rainbow trout (*Oncorhynchus mykiss*). *Canadian Journal of Fisheries and Aquatic Sciences*, *65*, 1060–1075.

Elsdon, T. S., Ayvazian, S., McMahon, K. W., & Thorrold, S. R. (2010). Experimental evaluation of stable isotope fractionation in fish muscle and otoliths. *Marine Ecology Progress Series*, *408*, 195–205.

Faure, G., & Mensing, T. M. (2004). *Isotopes: Principles and applications* (p. 928). John Wiley & Sons Inc.

Fisher, C. M., Paton, C., Pearson, D. G., Sarkar, C., Luo, Y., Tersmette, D. B., & Chacko, T. (2017). Data Reduction of Laser Ablation Split-Stream (LASS) Analyses Using Newly Developed Features Within Iolite: With Applications to Lu-Hf + U–Pb in Detrital Zircon and Sm-Nd + U–Pb in Igneous Monazite. *Geochemistry, Geophysics, Geosystems*, *18*, 4604–4622.

Hamilton, V., & Evans, K. (2018). Establishing growth chronologies from marine mammal teeth: A method applicable across species. *Journal of Experimental Marine Biology and Ecology*, *505*, 24–34.

Hegg, J. C., Fisher, C. M., & Vervoort, J. (2020). Simultaneous determination of 87Sr/86Sr and trace-element data in otoliths and other sclerochronological hard structures. *bioRxiv*. https://doi.org/10.1101/2020.04.24.060640

Hegg, J. C., Graves, B., & Fisher, C. M. (2021). Sawfish, read in tooth and saw: Rostral teeth as endogenous chemical records of movement and life-history in a critically endangered species. *Aquatic Conservation: Marine and Freshwater Ecosystems*, *31*, 2334–2347.

Hegg, J. C., Kennedy, B. P., & Chittaro, P. M. (2018). What did you say about my mother? The complexities of maternally derived chemical signatures in otoliths. *Canadian Journal of Fisheries and Aquatic Sciences*, *76*, 81–94.

Hegg, J. C., Kennedy, B. P., Chittaro, P. M., & Zabel, R. W. (2013). Spatial structuring of an evolving life-history strategy under altered environmental conditions. *Oecologia*, *172*, 1017–1029.

Hegg, J. C., Kennedy, B. P., & Fremier, A. K. (2013). Predicting strontium isotope variation and fish location with bedrock geology: Understanding the effects of geologic heterogeneity. *Chemical Geology*, *360–361*, 89–98.

Janak, J. M., Linley, T. J., Harnish, R. A., & Shen, S. D. (2021). Partitioning maternal and exogenous diet contributions to otolith 87Sr/86Sr in kokanee salmon (*Oncorhynchus nerka*). *Canadian Journal of Fisheries and Aquatic Sciences*, *78*, 1146–1157.

Johnson, R. C., Weber, P. K., Wikert, J. D., Workman, M. L., MacFarlane, R. B., Grove, M. J., & Schmitt, A. K. (2012). Managed metapopulations: Do Salmon hatchery 'sources' lead to in-river 'sinks' in conservation? *PLoS ONE*, *7*, e28880.

Kalish, J. M. (1990). Use of otolith microchemistry to distinguish the progeny of sympatric anadromous and non-anadromous salmonids. *Fishery Bulletin*, *88*, 657–666.

Kennedy, B., Blum, J., Folt, C., & Nislow, K. (2000). Using natural strontium isotopic signatures as fish markers: Methodology and application. *Canadian Journal of Fisheries and Aquatic Sciences*, *57*, 2280–2292.

Kennedy, B., Folt, C., Blum, J., & Chamberlain, C. (1997). Natural isotope markers in salmon. *Nature*, *387*, 766–767.

Killick, R., & Eckley, I. A. (2014). Changepoint: An R package for changepoint analysis. *Journal of Statistical Software*, *1*(3), 1–19.

Kurle, C. M., & Gudmundson, C. J. (2007). Regional differences in foraging of young-of-the-year Steller Sea lions *Eumetopias jubatus* in Alaska: Stable carbon and nitrogen isotope ratios in blood. *Marine Ecology Progress Series*, *342*, 303–310.

Limburg, K. E., Walther, B. D., Lu, Z., Jackman, G., Mohan, J., Walther, Y., Nissling, A., Weber, P. K., & Schmitt, A. K. (2015). In search of the dead zone: Use of otoliths for tracking fish exposure to hypoxia. *Journal of Marine Systems*, *141*, 167–178.

Michibata, H., & Hori, R. (1979). The accumulation of manganese from the environmental medium by the egg of *Oryzias latipes*. *Journal of Cellular Physiology.*, *98*, 241–244.

Miller, J. A., Butler, V. L., Simenstad, C. A., Backus, D. H., & Kent, A. J. R. (2011). Life history variation in upper Columbia River Chinook salmon (*Oncorhynchus tshawytscha*): A comparison using modern and ~500-year-old archaeological otoliths. *Canadian Journal of Fisheries and Aquatic Sciences*, *68*, 603–617.

Miller, J. A., & Kent, A. J. R. (2009). The determination of maternal run time in juvenile Chinook salmon (*Oncorhynchus tshawytscha*) based

on Sr/ca and 87Sr/86Sr within otolith cores. *Fisheries Research*, *95*, 373–378.

Mohan, J. A., Miller, N. R., Herzka, S. Z., Sosa-Nishizaki, O., Kohin, S., Dewar, H., Kinney, M., Snodgrass, O., & Wells, R. J. D. (2018). Elements of time and place: Manganese and barium in shark vertebrae reflect age and upwelling histories. *Proceedings of the Royal Society B: Biological Sciences*, *285*, 20181760. https://doi.org/10.1098/rspb.2018.1760

Oakerman, A., Bumgarner, J., Golden, S., & Fortier, J. (2020). *Lyons ferry hatchery evaluations: Fall Chinook Salmon annual report*. Washington Department of Fish and Wildlife http://www.fws.gov/lsnakecomplan/reports/WDFWreports.html

Paton, C., Hellstrom, J., Paul, B., Woodhead, J., & Hergt, J. (2011). Iolite: Freeware for the visualisation and processing of mass spectrometric data. *Journal of Analytical Atomic Spectrometry*, *26*, 2508–2518.

R Core Team. (2021). *R: A language and environment for statistical computing*. R Foundation for Statistical Computing https://www.R-project.org/

Ruttenberg, B. I., Hamilton, S. L., Hickford, M. J. H., Paradis, G. L., Sheehy, M. S., Standish, J. D., Ben-Tzvi, O., & Warner, R. R. (2005). Elevated levels of trace elements in cores of otoliths and their potential for use as natural tags. *Marine Ecology Progress Series*, *297*, 273–281.

Schell, D. M. (2000). Declining carrying capacity in the Bering Sea: Isotopic evidence from whale baleen. *Limnology and Oceanography*, *45*, 459–462.

Steel, E. A., Tillotson, A., Larsen, D. A., Fullerton, A. H., Denton, K. P., & Beckman, B. R. (2012). Beyond the mean: The role of variability in predicting ecological effects of stream temperature on salmon. *Ecosphere*, *3*, 1–11.

Stevenson, D. K., & Campana, S. E. (1992). Otolith microstructure examination and analysis. *Canadian Special Publication of Fisheries and Aquatic Sciences*, *117*, 126p.

Stickney, R. R. (1991). *Culture of salmonid fishes*. CRC Press.

U.S. Fish and Wildlife Service. (1995). *Fisheries: fish health operations*. USFWS, FWM 170, Part 713 FW, Washington, DC.

Volk, E. C., Blakley, A., Schroder, S. L., & Kuehner, S. M. (2000). Otolith chemistry reflects migratory characteristics of Pacific salmonids: Using otolith core chemistry to distinguish maternal associations with sea and freshwaters. *Fisheries Research.*, *46*, 251–266.

Waite, E. M., Closs, G. P., Kim, J., Barry, B., Markwitz, A., & Fitzpatrick, R. (2008). The strontium content of roe collected from spawning brown trout *Salmo trutta* L. reflects recent otolith microchemistry. *Journal of Fish Biology*, *72*, 1847–1854.

Walther, B. D. (2019). The art of otolith chemistry: Interpreting patterns by integrating perspectives. *Marine and Freshwater Research*, *70*, 1643–1658.

Walther, B. D., & Thorrold, S. R. (2008). Continental-scale variation in otolith geochemistry of juvenile American shad (*Alosa sapidissima*). *Canadian Journal of Fisheries and Aquatic Sciences*, *65*, 2623–2635.

Zhang, Z., Beamish, R. J., & Riddell, B. E. (1995). Differences in otolith microstructure between hatchery-reared and wild Chinook Salmon (*Oncorhynchus tshawytscha*). *Canadian Journal of Fisheries and Aquatic Sciences*, *52*, 344–352.

Zimmerman, C. E. (2005). Relationship of otolith strontium-to-calcium ratios and salinity: Experimental validation for juvenile salmonids. *Canadian Journal of Fisheries and Aquatic Sciences*, *62*, 88–97.

SUPPORTING INFORMATION

Additional supporting information can be found online in the Supporting Information section at the end of this article.

How to cite this article: Chittaro, P., Hegg, J., Fuhrman, A., Robichaux, D., Doung, R., Beckman, B., Fisher, C., Vervoort, J., & Kennedy, B. (2023). The incorporation of environmentally derived $^{87}Sr/^{86}Sr$ and Sr/Ca in early otolith formation of Chinook salmon. *Ecology of Freshwater Fish*, *32*, 107–119. https://doi.org/10.1111/eff.12673